THE JOURNAL OF PHYSICAL CHEMISTRY C

Article

Intrinsic Chirality in Bare Gold Nanoclusters: The Au$_{\bar{}}$ Case

Itzel E. Santizo, Francisco Hidalgo, Luis A. Pe#rez, Cecilia Noguez, and Ignacio L. Garzo#n

J. Phys. Chem. C, **2008**, 112 (45), 17533-17539 • DOI: 10.1021/jp806080b • Publication Date (Web): 16 October 2008

Intrinsic Chirality in Bare Gold Nanoclusters: The Au_{34}^- Case

Itzel E. Santizo, Francisco Hidalgo, Luis A. Pérez, Cecilia Noguez, and Ignacio L. Garzón*

Instituto de Física, Universidad Nacional Autónoma de México, Apartado Postal 20-364, 01000 México D. F., México

Received: July 9, 2008; Revised Manuscript Received: August 10, 2008

In this work, we provide theoretical evidence on the existence of energetically stable chiral structures for bare gold clusters. Density functional theory calculations within the generalized-gradient approximation were performed to systematically study structural, vibrational, electronic, and optical properties of the lowest-lying isomers of the Au_{34}^Z, ($Z = +1, 0, -1$), clusters. Our results show that for the neutral and charged clusters, the lowest-energy isomer has a C_1 (chiral) structure. In addition, a C_3 (chiral) isomer was found nearly degenerate in energy with the C_1 isomer. These results are in agreement with previous theoretical-experimental studies done for the Au_{34}^- cluster; however, because our calculated molecular scattering functions for the C_1 and C_3 isomers of this cluster are almost indistinguishable, it is concluded that the actual resolution in trapped ion electron diffraction experiments is not enough to discriminate between them. On the other hand, the electronic density of states of the C_1 isomer shows better overall agreement with the measured photoelectron spectrum of the Au_{34}^- cluster than that one corresponding to the C_3 isomer. The electronic density of states of these isomers also shows different features in the energy region of the HOMO−LUMO gap, which would generate distinct behavior in their optical properties. In fact, the calculated absorption and circular dichroism spectra of the two chiral isomers show clear differences in their line shape. Another important property that distinguishes the C_1 and C_3 isomers is the different spatial distribution of the atomic coordination on the cluster surface. Our results confirm that the potential energy surface of bare gold clusters could have lowest-lying energy minima corresponding to intrinsically chiral structures.

Introduction

The theoretical and experimental study of energetically stable structures of gold clusters is an important and very active field of research.[1] By combining techniques like cluster ion mobility (CIM),[2] photoelectron spectroscopy (PES),[3,4] and trapped ion electron diffraction (TIED),[5] with density functional theory (DFT) calculations, interesting trends on the structural motifs of the lowest-energy isomers of gold clusters have been reported. For example, for anionic Au_n^- clusters with $n < 13$, 2D structures were proposed,[3,5] whereas for $n = 16-18$ empty cage-like structures[6] have been detected. A perfect tetrahedron for the Au_{20}^- cluster,[7] and tetrahedral-based structures[5,8,9] for $n = 21-23$ have also been reported. For Au_{24}^-, a hollow tubular structure was proposed,[5,8,9] but, interestingly, only up to $n = 25$ a core−shell structure with a single core atom was obtained.[9]

Another interesting case is the Au_{32} neutral cluster with an I_h cage-like structure that was theoretically predicted as the lowest-energy isomer;[10,11] however, PES measurements on the Au_{32}^- cluster, taken at room temperature, indicated that a low-symmetry compact C_1 isomer fits best the experimental data.[12] A recent theoretical study[13] showed that, although the lowest-energy structure of the Au_{32} neutral cluster indeed corresponds to the I_h cage-like structure, the energetic ordering of the lowest-lying isomers change for the anionic Au_{32}^- cluster. In that study,[13] a systematic search of the lowest-energy minima was performed combining a global optimization technique (genetic algorithms) and a many-body Gupta potential with a further local minimization, using DFT calculations within the generalized-gradient approximation (GGA). The results obtained showed that the lowest-energy isomer of the Au_{32}^- cluster corresponds to a low-symmetry C_1 compact structure, indicating that a single additional charge is enough to modify the energetic ordering of the neutral cluster isomers.[13] This study also predicts that low-symmetry disordered structures, for both the Au_{32}^- and the Au_{32}^+ clusters, should be detected not only at room temperature as was experimentally verified for the Au_{32}^- case[12] but also at much lower temperatures.[13]

The search for the most stable structure of the large-band gap (0.94−0.96 eV) Au_{34}^- cluster has also received special attention recently.[14,15] In a theoretical-experimental study, combining PES, TIED, and time-dependent DFT calculations, it was suggested that an isomer with C_3 (chiral) point symmetry is the most abundant in the investigated ensemble of size-selected clusters.[14] In other work, the structural and electronic properties of the Au_{34}^- cluster were also investigated using accurate theoretical calculations and PES.[15] In contrast with the former study,[14] in the latter one, it was concluded that a disordered-fluxional isomer with C_1 point symmetry is the most likely candidate responsible of the PES data.[15] In both studies,[14,15] it was also found that there are other lowest-lying isomers very close in energy with respect to either the C_3 or the C_1 isomers, but after a data analysis it was concluded that they only provide minor contributions to the TIED[14] and PES[14,15] spectra. The lack of agreement in the structure determination of the isomers of the Au_{34}^- cluster that makes the major contribution to the TIED[14] and PES[14,15] data is surprising since both studies used *state of the art* experimental techniques in conjunction with accurate quantum mechanical calculations. On the other hand, although the C_3 and C_1 isomers belong to different rotational symmetry groups, and therefore they are structurally different,

* To whom correspondence should be addressed. E-mail: garzon@fisica.unam.mx. Phone: +52-55-56225147. Fax: +52-55-561651535.

10.1021/jp806080b CCC: $40.75
Published on Web 10/16/2008

it is appealing that both isomers, by definition,[16] correspond to metallic chiral nanostructures.

Chirality in bare and thiolate-passivated gold clusters had been studied before[17−19] to provide theoretical insights into the physicochemical origin of the giant optical activity measured on glutathione-passivated gold clusters[20] and on other related systems.[21] The study of the enantiospecific adsorption of a chiral amino acid on a chiral Au_{55} cluster[22] has also shown the relevance and possible applications of chiral gold clusters. It is, therefore, encouraging the existence of experimental evidence of chiral structures for the bare Au_{34}^- cluster, with either C_3 or C_1 rotational symmetry group.

In this work, we provide additional theoretical evidence on the existence of energetically stable (lowest-lying local minima of the potential energy surface) chiral structures for the Au_{34}^Z, ($Z = +1, 0, -1$), clusters, by studying their structural, vibrational, electronic, and optical properties, using DFT−GGA calculations. This study is useful by itself and also because, as mentioned above, there is not yet agreement in the structure determination of the Au_{34}^- cluster after combining TIED, PES, and theoretical calculations.[14,15] Our results show that for the neutral and charged clusters, the lowest-energy isomer is a disordered C_1 (chiral) structure. This C_1 isomer corresponds to the structure first reported in ref 15, which is the main contributor to the measured PES spectra of the Au_{34}^- cluster. For the Au_{34}^- cluster, we also obtained that the C_3 isomer, first reported in ref 14, is nearly degenerate in energy with the C_1 isomer (our calculated total energy difference is: 0.031 eV). Because the theoretical calculated molecular scattering functions of the two chiral structures are very similar, we conclude that the present resolution of the TIED technique is not enough to clearly discriminate between the C_1 and C_3 isomers of the Au_{34}^- cluster. On the other hand, the calculated electronic density of states (DOS) of the C_1 isomer is in better agreement with the measured photoelectron spectrum than that one corresponding to the C_3 structure. The DOS of both chiral isomers show major differences, particularly in the HOMO−LUMO energy gap region, which will affect differently the optical behavior of them. To confirm this hypothesis, we have calculated the absorption and circular dichroism (CD) spectra of the C_1 and C_3 isomers. Our results confirm that these isomers are intrinsically chiral because the calculated CD spectra of both isomers are different from zero, but their line shape is not the same, implying that they respond differently to the interaction with circularly polarized light. Our results also show that another important property that distinguishes the C_1 and C_3 isomers is the different atomic coordination on the cluster surface, which may produce distinct enantiospecific patterns when they interact with chiral molecules.[22] Overall, our present calculations confirm the existence of intrinsic chiral Au_{34}^- cluster isomers corresponding to lowest-lying minima of its potential energy surface.

Computational Methods

The structural optimization of the gold clusters presented herein was performed following a procedure similar to that reported in previous publications by our group.[13,17,18,22−25] At the last stage of the calculations, the cluster structures were optimized by unconstrained relaxations using the forces calculated from DFT. The DFT−GGA calculations were performed with the *SIESTA* code[26] using scalar relativistic norm-conserving pseudopotentials,[27] a double-ζ basis set,[13,22,25] and the Perdew−Burke−Ernzerhof (PBE) parametrization.[28] For the cluster structure optimization, a force tolerance of 0.01 eV/Å was used; whereas for the vibrational frequencies calculation this value was decreased to 0.001 eV/Å. This methodology has been used before to study the trends in the structure and bonding of noble metal clusters.[13,25,29] In particular, the energetic, structural, and electronic properties of neutral and charged Au_n, ($n = 2-13$) clusters, as well as the relative stability of the Au_{20} and Au_{32} clusters were studied using the same level of approximation as mentioned above,[13,25,29] obtaining good agreement with other theoretical studies and with experimental data, when they were available. For example, the DFT−GGA−PBE methodology we utilized in the present calculations had been used before to investigate the most stable configuration of the neutral Au_8 cluster.[25,29] The results obtained indicate that the capped square planar structure is the most-stable one,[25,29] in agreement with the high-level correlation wave function data recently reported by Olson and Gordon.[30] Although we consider that the conclusions obtained in the above-mentioned studies on smaller noble metal clusters[13,25,29] justify the use of the same methodology for the investigation of structural properties of neutral and charged Au_{34} clusters, it is important to mention that questions related to the use of other exchange-correlation functionals, spin-polarization calculations, and effects due a larger basis set or spin−orbit coupling have not been considered in the present work. Instead, a systematic search for the most stable configurations of neutral and charged Au_{34} clusters was attempted by performing local structural relaxations using DFT−GGA−PBE forces on the cluster geometries obtained from a global optimization procedure, combining genetic algorithms and a semiempirical many-body potential.[13,17,18,22−24]

The chiroptical properties of the C_1 and C_3 isomers of the Au_{34}^- cluster were theoretically studied by calculating their CD and optical absorption spectra. In particular, the electronic CD spectrum was evaluated from the Rosenfeld equation[31] for the rotational strength: $G_{\alpha\beta}(\omega) = -2/\hbar\, Im \sum_{n\neq 0} \omega \langle\psi_0|\mu_\alpha|\psi_n\rangle\langle\psi_n|m_\beta|\psi_0\rangle / \omega_{n0}^2 - \omega^2$, where *Im* denotes the imaginary part of the scalar product of the matrix elements $\boldsymbol{\mu}^{0n}{}_\alpha$ and $\mathbf{m}^{n0}{}_\beta$ of the respective Cartesian components of the electric and magnetic dipole moments that correspond to a transition from the ground state ψ_0 to the excited state ψ_n, and ω is the frequency of the incident radiation field, which is circularly polarized. The trace of G is proportional to the CD signal, which is given by the difference of the molar extinction ($\Delta\epsilon$) between left- and right-circularly polarized light.[31] Here, we consider electronic transitions over all occupied and unoccupied states, generated by the extended-function basis set that assures convergence of the chiroptical effects. During the past few years, considerable progress has been made to perform direct calculations of optical rotatory strengths based on the evaluation of matrix elements of both electric and magnetic transition moments using advanced quantum descriptions of the molecular excited states like time-dependent DFT (TDDFT).[32] Nevertheless, this methodology suffers the lack of precision by problems with the basis set completeness and with the treatment of dynamic electron correlation,[33] and on the other hand, is still unpractical to study the chiroptical properties of gold clusters with the size of interest in this work, due the huge computational effort involved. In this work, we follow an alternative approach incorporating the appropriate quantum mechanical expressions, based on time-dependent perturbation theory, to calculate the CD and optical absorption spectra within the framework of the *SIESTA* program.[34] Within this approach the matrix elements of the electric and magnetic dipole transition moments were calculated using as final states, the unoccupied molecular orbitals generated by the partially occupied 6s and polarization 6p orbitals forming the basis set.[35] This methodology has been tested for several

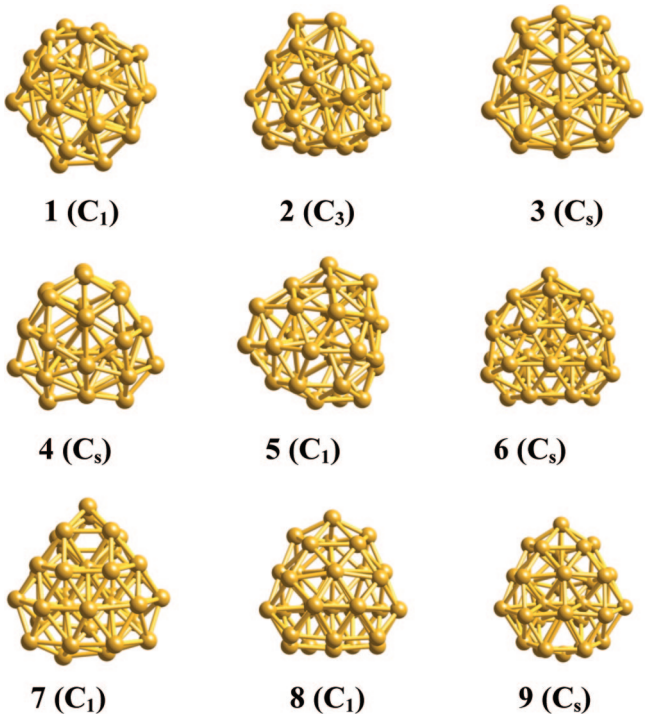

Figure 1. Optimized geometries for the Au_{34}^- clusters obtained at the DFT−GGA−PBE level of theory.

TABLE 1: Table 1

isomer	Au_{34}^-	HCM	isomer	Au_{34}	isomer	Au_{34}^+
1	0.000	0.115	1	0.000	1	0.000
2	0.031	0.121	4	0.134	2	0.170
3	0.080	0.004	5	0.161	3	0.184
4	0.099	0.007	3	0.181	4	0.187
5	0.144	0.102	2	0.182	6	0.280
6	0.152	0.006	6	0.222	7	0.415
7	0.355	0.089	8	0.600	5	0.469
8	0.491	0.018	7	0.607	8	0.494
9	0.638	0.006	9	0.801	9	0.538

carbon nanotubes[34] and chiral molecules and fullerenes[35] like C_{76} and C_{84}, obtaining good agreement with previous TDDFT calculations and experimental results.[34,35]

Results and Discussion

The structural optimization of the Au_{34}^Z ($Z = -1, 0, 1$) clusters, using the DFT−GGA methodology described above, allows us to obtain the isomers with the lowest total energy, which would correspond to the most stable cluster structures. The nine isomers with the lowest energy we obtained for the Au_{34}^- cluster are displayed in Figure 1,[36] whereas the corresponding relative total energies are presented in Table 1. The lowest energy isomer we found for the Au_{34}^- cluster is that one with C_1 (chiral) point symmetry. This structure was first obtained by Gu et al.,[15] using a basin-hopping global optimization technique combined with the DFT−GGA method. An interesting result from the present study is that the same C_1 isomer is also the most stable configuration for the neutral Au_{34} and cationic Au_{34}^+ clusters. This is in contrast with the trend we obtained in the study of the structural properties of the Au_{32}^Z, ($Z = -1, 0, 1$), clusters, where the most stable isomer for the neutral Au_{32} cluster is the I_h cagelike isomer, whereas for the anionic and cationic Au_{32} clusters, a C_1 structure is the most stable one.[13] Table 1 also shows the relative total energies of the neutral Au_{34} and cationic Au_{34}^+ cluster isomers taking as reference, like in the case of the anionic case, the total energy of the corresponding most stable C_1 isomer.

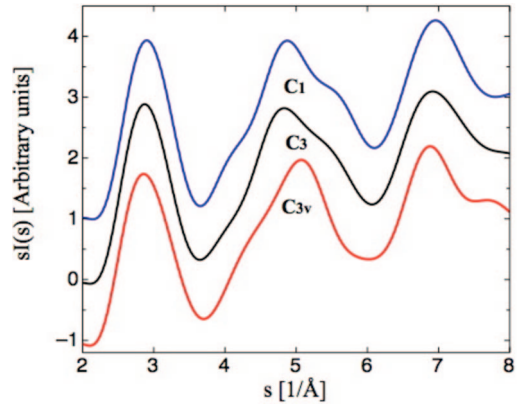

Figure 2. Calculated molecular scattering function for the C_1 (blue), C_3 (black), and C_{3v} (red) isomers of the Au_{34}^- cluster.

For the anionic Au_{34}^- cluster, an isomer with C_3 (chiral) point symmetry, isomer 2, was found nearly degenerate in energy ($\Delta E = 0.031$ eV) with the C_1 isomer. Isomer 2 is also the second one in the energy ordering for the cationic Au_{32}^+ cluster, but the difference in energy with the C_1 isomer is higher ($\Delta E = 0.170$ eV); whereas for the neutral case, it is the fifth isomer, 0.181 eV higher in energy. The C_3 isomer was first reported in ref 14 as the most stable isomer for the Au_{34}^- cluster after a limited structural optimization using DFT; whereas in ref 15 it was found as the third isomer in the energy ordering.

The relative total energies shown in Table 1 indicate that the energy ordering of the nine lowest-lying isomers is the same for the anionic and cationic 34 atom gold clusters, but in the case of the neutral cluster, these isomers are distributed in a different way. This result, also found in the structural optimization of the Au_{32}^Z, ($Z = -1, 0, 1$), clusters,[13] confirms the trend that the addition or subtraction of a single charge on a neutral gold cluster with as many as 34 atoms could be enough to modify the energy ordering of their isomers.

The geometries of isomers 3−9 of the Au_{34}^- clusters displayed in Figure 1 correspond to low-symmetry and chiral structures. Isomers 3, 4, 6, and 9 only have a single plane of symmetry (C_s point symmetry) and isomers 5, 7, and 8 have no symmetry at all (C_1 point symmetry). The four isomers with C_s point symmetry are achiral whereas the remaining 3 isomers with C_1 point symmetry are chiral. One way to quantify, from a geometrical point of view, the index of chirality of these isomers is through the Hausdorff chirality measure (HCM), which was introduced in refs 17−19. The calculated HCM values for the 9 isomers of the Au_{34}^- cluster are displayed in Table 1. As expected, the HCM values for the four achiral isomers are almost equal to zero, whereas the C_3 isomer has the largest index of chirality. The energetic predominance of chiral and low-symmetry structures for the lowest-lying isomers of gold clusters around the present size is another emerging trend that from this and other related calculations can now be firmly established.

The results discussed above on the energetic ordering of the most stable isomers of the Au_{34}^- cluster are in good agreement with those obtained by Gu et al.[15] In particular, we confirmed that the C_1 isomer is the lowest-energy one, and, therefore, the best candidate for the global minimum, as it was suggested in ref 15. On the other hand, this isomer was not considered for the interpretation of the TIED and PES spectra in ref 14, but it was suggested that the C_3 isomer fits better both sets of experimental data.[14] Because the C_1 isomer was found to be

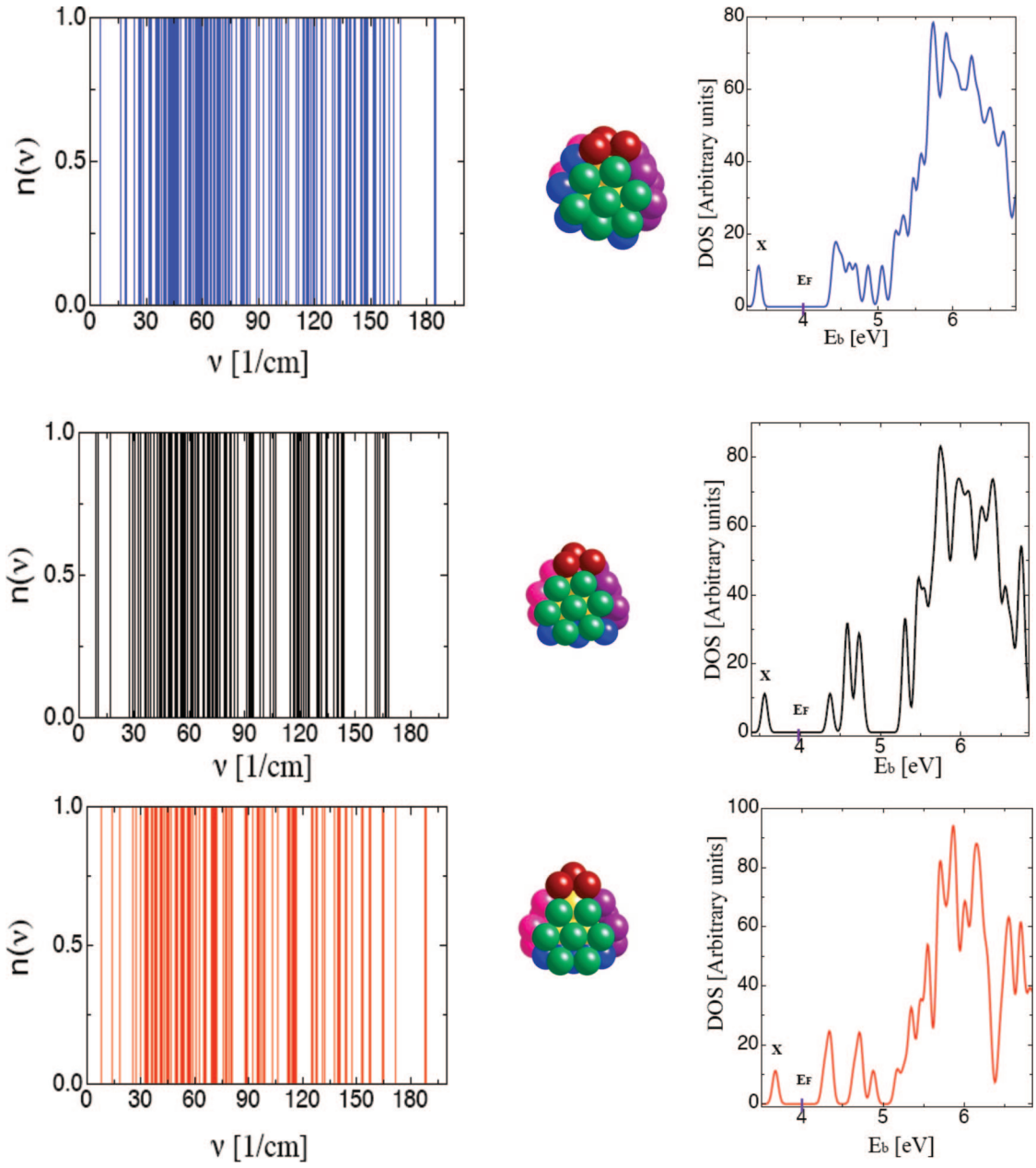

Figure 3. Distribution of vibrational frequencies (left column) and electronic density of states (right column) for the C_1 (blue), C_3 (black), and C_{3v} (red) isomers of the Au_{34}^- cluster. A Gaussian broadening of 0.1 eV was used for the electronic density of states. The structures of these three isomers are shown in the middle column, displaying their hexagonal facets with different colors.

the most stable one, it is appropriate to investigate to what extent this isomer would fit the TIED data reported in ref 14. Figure 2 shows the calculated molecular scattering function for the C_1 and C_3 isomers, together with the corresponding curve of a 34 atom gold anionic cluster with C_{3v} (fcc) point symmetry,[37] which we included as a useful reference, despite this isomer with higher symmetry is 0.96 eV higher in energy with respect to the C_1 isomer. A careful analysis of the curves displayed in Figure 2 indicates that the molecular scattering functions of the C_1 and C_3 isomers are almost indistinguishable, whereas the corresponding curve of the C_{3v} isomer shows slight differences. For a quantitative comparison of these curves, we calculated the weighted profile factor R_w[14] of the theoretical molecular scattering functions with respect to the experimental TIED data reported in ref 14. The calculated R_w values (with w = 1.0) are 3.8, 3.9, and 6.2% for the C_1, C_3, and C_{3v} isomers, respectively. The corresponding R_w value for the difference between the two theoretical molecular scattering functions of the C_1 and C_3 isomers is 3.6%. These results imply that the atomic structure of the C_1 isomer fits the TIED data as well as the C_3 isomer does, and therefore both isomers need to be considered as responsible for the TIED data. The present analysis also indicates that the TIED technique is providing sort of averaged cluster structural information, which in this case it is not enough to discriminate between the geometrically different C_1 and C_3 isomers.

We have shown that the chiral C_1 and C_3 isomers of the Au_{34}^- cluster are nearly degenerate in energy and their molecular scattering functions are almost indistinguishable; however, other physical properties like the vibrational and electronic density of states look very different for these isomers. Figure 3 shows these quantities for the C_1 and C_3 isomers as well as for the C_{3v} one. As expected for coinage metal clusters of the present size, the values of the harmonic frequencies extend from around 15 to 190 cm^{-1} with clear differences between the three isomers in how they are distributed along this frequency range. For example, the existence of higher frequency modes and a more

evenly distribution of normal modes is characteristic of the C_1 isomer with respect to C_3 one. These differences in the vibrational frequencies of chiral isomers of the Au_{34}^- cluster would be relevant if they can be coupled with the low-frequency modes of chiral molecules adsorbed on them, such that the corresponding frequency shifts and line broadening could be detected using, for example, vibrational circular dichroism.[38] The vibrational frequencies were used to calculate the zero-point energy contribution and the free energy in the harmonic approximation to analyze if there is any change in the energy ordering between the C_1 and C_3 isomers. Our results indicated that the C_1 remains as the most stable one in a broad range of temperatures (at least up to 500 K).

The calculated electronic density of states (DOS), obtained from the Kohn−Sham eigenvalues, is also displayed in Figure 3 for the C_1, C_3, and C_{3v} isomers of the Au_{34}^- cluster. We found excellent agreement with the theoretically simulated PES spectra of the C_1 and C_3 isomers reported in ref 15 confirming the reliability of our DFT−GGA methodology. This agreement is not only obtained for the overall spectral patterns but also for the values of the HOMO−LUMO energy gaps. Our calculated values for these energy gaps are: 0.99 eV (C_1), 0.81 eV (C_3), and 0.58 eV (C_{3v}). As was discussed in ref 15 because the DOS of the C_1 isomer shows better overall agreement with the PES experiment than the corresponding DOS of the C_3 isomer, we confirm that the most likely candidate responsible of the observed PES would be the C_1 chiral isomer.

The different features of the DOS exhibited by these isomers, in particular around the region of the HOMO−LUMO gap, may also be detected through optical spectroscopy. Figure 4 shows the optical absorption (upper panels) and CD spectra (lower panels) for the (a) C_1, (b) C_3, and (c) C_{3v} isomers. The electronic transitions from occupied to unoccupied molecular-like states start at about 0.9, 0.8, and 0.6 eV for the C_1, C_3, and C_{3v} isomers respectively, in consistency with the calculated HOMO−LUMO energy gaps. Moreover, the absorption spectra show well-defined features for each isomer. For instance, whereas the spectrum of the C_{3v} isomer shows sharp peaks at 0.65, 0.95, and 1.35 eV (part c of Figure 4), the spectrum of C_1 shows a continue band from 1 to 2.5 eV (part a of Figure 4). On the other hand, the absorption spectrum of the C_3 isomer shows an intermediate behavior between C_1 and C_{3v} because it shows a small peak at 1.25 eV and a more intense peak at 1.9 eV, where a continue band starts, and finishes at about 2.2 eV (part b of Figure 4). The characteristic peaks in the optical absorption spectrum of the C_{3v} isomer are due to electronic transitions associated to the degenerate molecular-like electronic states (Figure 3). This degeneracy is originated from the arrangement of the atoms in this highly symmetric cluster. When the atomic symmetry is broken, the degeneracy is lost and the molecular-like electronic states are close enough such that the electronic transitions form optical bands, as observed in the spectrum of the C_1 isomer. This behavior can also be observed in the DOS shown in Figure 3 for the 3 isomers. In the case of the C_{3v} isomer, the DOS shows well-defined peaks due to occupied and unoccupied states close to the Fermi level. On the other hand, the occupied states of the C_1 isomer form a band, whereas the C_3 isomer shows an intermediate behavior, where the occupied states are not close enough to form a band, but also they are not far apart to show single peaks.

The origin of the optical spectra can be understood in terms of the calculated Kohn−Sham atomic orbitals within the DFT scheme used for the anionic isomers. For the three isomers, the states around the HOMO are mainly composed of 5d and 6s

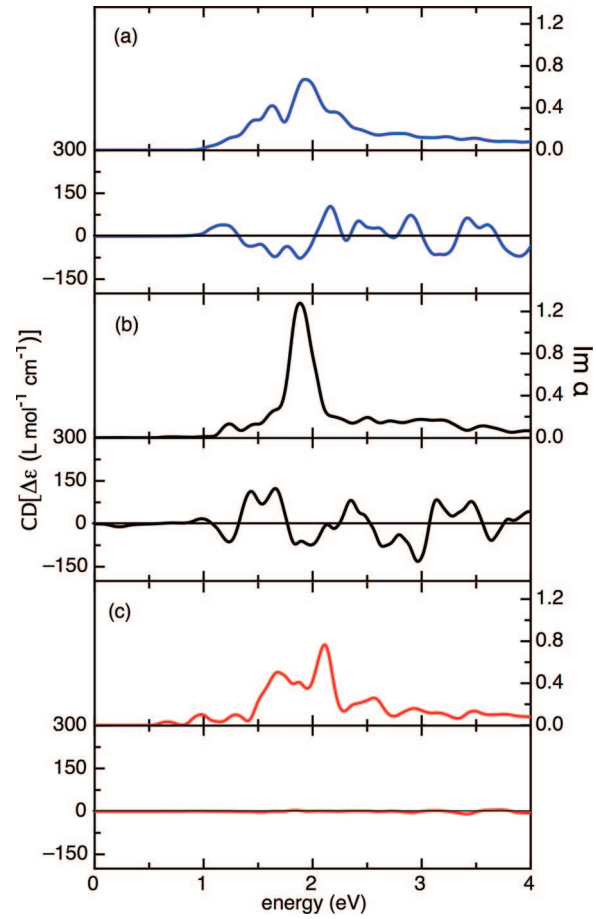

Figure 4. Imaginary part of the polarizability per volume unit (upper panels) and circular dichroism spectra (lower panels) of the (a) C_1 (blue), (b) C_3 (black), and (c) C_{3v} (red) isomers of the Au_{34}^- cluster. A Gaussian broadening of 0.05 eV was employed for all of the spectra. The relation between the theoretical expression for the rotational strength given in the text, and the calculated CD values reported in Figure 4 are discussed in the Supporting Information section. In the units of $\Delta\epsilon$ for the CD curves, L means liters.

orbitals with small 6p orbital contributions, whereas above 5 eV in the DOS, the 5d orbitals dominate the occupied molecular-like states (Figures SP1 and SP2 in the Supporting Information). The lowest LUMO states, below 4 eV in the DOS (Figures SP1 and SP2), are mainly composed of 6s orbitals, whereas the contribution of 5d and 6p orbitals is less important. Thus, the optical absorption at low energies mainly comes from molecular-like electronic transitions from 6s to 5d and 6p orbitals, and some contributions from the transitions from 5d to 6s and 6p orbitals. Above 3 eV, all of the absorption spectra show a tail due to electronic transitions from 5d to 6s and 6p electron states, mainly. The main features of our calculated optical spectra agree quite well with experiments and other calculations for similar structures like thiolate-protected Au_{25} [39,40] and Au_{38}.[41] Notice that for the three isomers, strong quantum size effects are still present, with the cluster symmetry determining the energy location of the molecular-like electronic states, and the optical signature of each cluster. In contrast, gold nanoparticles have electronic bands, and collective electron excitations known as surface plasmon resonances are present.

To corroborate the relationship between the optical response and the chiral cluster structure, the CD spectra of these isomers were calculated. The bottom panels of parts a, b, and c of Figure 4 show these spectra for the C_1, C_3, and C_{3v} isomers, respectively. As expected, the C_{3v} isomer does not show any

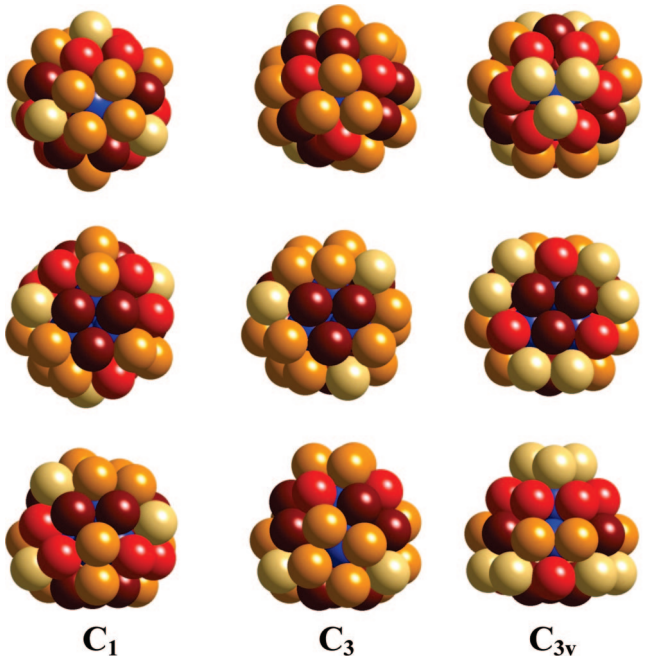

Figure 5. Atomic coordinations of the C_1 (left column), C_3 (middle column), and C_{3v} (right column) isomers of the Au_{34}^- cluster. The color of the spheres indicates different values of the atomic coordination N_c: beige ($N_c = 5$), orange ($N_c = 6$), red ($N_c = 7$), maroon ($N_c = 8$), blue ($N_c = 12$).

optical activity because it has a vertical mirror symmetry plane. On the other hand, C_1 and C_3 isomers exhibit CD due to their intrinsic chirality. The optical activity of the C_3 isomer starts at about 0.9 eV, and its first prominent peak at 1.25 eV is negative, which is related with the first electronic transition observed in absorption. Then, two positive peaks are present at 1.4 and 1.65 eV, which would be associated to electronic transitions from 5d to 6s orbitals and from 5d to 6p orbitals. Then, the next structure is negative again and is related to the intense absorption peak at 1.9 eV. At higher energies, the CD continues changing in sign in an alternate way, where the main electronic transitions, that give rise the absorption spectrum are present. Contrary to C_3, the CD spectrum of C_1 begins with a positive peak at 1.2 eV, then a negative structure composed of three peaks at 1.4, 1.6, and 1.9 eV is present. Again, these peaks would be related with the electronic transitions at from 5d to 6s orbitals, and from 5d to 6p orbitals. Also, at higher energies, the CD continues changing in sign in an alternate way, following the main electronic transitions of the absorption spectrum. In all cases, we have not found a correlation between the absorption intensity and the magnitude of the positive and negative peaks of the CD spectra because all of them exhibit more or less the same intensity. It should be noticed that the theoretically predicted CD spectra of these Au_{34}^- isomers are of the same magnitude as that one already measured in suspensions of chiral C_{84} fullerenes[42] using standard spectrometers.

Another important property that distinguishes the C_1 and the C_3 isomers of the Au_{34}^- cluster is the different spatial distribution of the atomic coordination on the cluster surface. Figure 5 shows three different views (top, bottom, and side) of the cluster geometries for these isomers together with that one for the C_{3v} one. The atomic coordination is displayed using different colors for the spheres representing the gold atoms. The color code for the atomic coordination is as follows: 5 (beige), 6 (orange), 7 (red), 8 (maroon), 12 (blue). As it was discussed in ref 24, the metallic bonding in gold clusters is characterized by preferring low-symmetry (disordered) structures over highly symmetric (ordered) geometries due to an increase in the atomic coordination and the contraction of the interatomic bond lengths at the cluster surface. This mechanism is clearly shown in Figure 5, where one can observe the smaller atomic coordination of the highly symmetric C_{3v} isomer (with average coordination number equal to 7.059) with respect to the higher atomic coordination existing in the energetically more stable chiral C_1 (with average coordination number equal to 7.235) and C_3 (with average atomic coordination equal to 7.118) isomers of the Au_{34}^- cluster. In fact, after a surface reconstruction of the C_{3v} isomer, it transforms to a C_3 one, lowering its total energy.[14,37] An additional deformation of this structure produces a further decrease of the cluster's energy, giving rise to the C_1 isomer. Although the isomers C_1 and C_3 are nearly degenerate in energy, the spatial distribution of the atomic coordination at their cluster surface shown in Figure 5, presents some differences. For example, isomer C_3 has a larger number of low-coordinated atoms (3 with coordination 5 and 15 with coordination 6) than the C_1 isomer (4 with coordination 5 and 12 with coordination 6). The difference in atomic coordination displayed at the cluster surface of these isomers is relevant because they would generate distinct catalytic activity and adsorption patterns through the interaction with organic molecules.[22]

Conclusions

The theoretical results reported in the present study, together with those obtained by combining DFT calculations with PES and TIED[14] and PES,[15] provide incontrovertible evidence on the existence of chiral structures for bare gold clusters. Specifically, we have shown that chiral isomers with C_1 and C_3 symmetry are nearly degenerate lowest-lying minima of the potential energy surface of the Au_{34}^- cluster. Furthermore, our calculated molecular scattering functions for both isomers are in good agreement with the data obtained from TIED[14] experiments realized on this cluster. On the other hand, our calculated electron DOS corresponding to the C_1 isomer is found to be in much better agreement with the PES spectrum measured for the Au_{34}^- cluster than that one calculated for the C_3 isomer, indicating that the chiral C_1 isomer is the main responsible of the PES data, as was also suggested in ref 15. From an energetic point of view, our calculations indicate that the C_1 isomer is slightly more stable than the C_3 one; however, the theoretical results reported in ref 15 show that the energy difference between both isomers could be larger in favor of the C_1 isomer. Overall, these results confirm that bare-gold clusters could have energetically stable isomers (lowest-lying minima of their potential energy surface), with intrinsically chiral structures. This conclusion is based on the well-established group theory concept that any aggregate of atoms with C_n ($n = 1, 2...$) point symmetry will be a chiral system.[16]

To provide additional insights into the chiroptical properties of the C_1 and C_3 chiral isomers of the Au_{34}^- cluster, we performed DFT−GGA−PBE calculations to obtain an initial knowledge of their optical absorption and CD spectra. Theoretical predictions of these optical properties are useful because it is expected that in the near future efficient enantiomeric separation methods could be developed to measure, for example, the optical activity of bare chiral gold clusters. In this direction, our study shows that, whereas the C_1 and C_3 structures cannot be discriminated using electron diffraction methods, their circular dichroism spectra are different enough to be distinguished through optical activity experiments; if indeed appropriate enantiomeric methods are implemented. Also, we consider that the present results will contribute to elucidate the physi-

cochemical origin of the optical activity measured in monolayer-protected gold nanoclusters using glutathione molecules[20] and other chiral ligands.[21,38,43−45] Because we have shown that bare gold clusters could be intrinsically chiral, the explanation that assumes a chiral metallic core as the main responsible of the optical activity measured in chiral-ligand-protected gold nanoparticles would be favored.

Finally, the question about which other clusters would be intrinsically chiral deserves some comments. For anionic gold clusters there is an increasing theoretical−experimental evidence indicating that the most stable structures of, for example, Au_{32}^-,[12,13] Au_{55}^-,[4,46] and Au_{56}^-−Au_{64}^-,[46] have low or null symmetry (C_1), and therefore they would be intrinsically chiral. Also, in several theoretical studies on the lowest-energy structures of neutral gold clusters the trend related with the highest energetic stability of disordered (C_1) isomers, is well established.,,[17−19 22−24 47−51] Another interesting example of a chiral gold cluster is the icosahedral (I symmetry) and spherically aromatic Au_{72} golden fullerene, which has been theoretically predicted as an isomer with high thermodynamic stability.[52] It is comfortable to know that the physical origin of the higher energetic stability of low symmetry and chiral cluster isomers has been already studied, and it was found to be related with the short-range of the n-body interactions[24,47−51] and the strong relativistic effects[1,4,25,46,52] existing in gold clusters. The real relevance of intrinsically chiral gold clusters for possible nanotechnological applications will depend on the development of not only better size and shape separation methods but also on the capability to separate enantiomers from racemic mixtures of chiral clusters with a given size and shape.

Acknowledgment. We acknowledge Prof. L. S. Wang for providing us with the x, y, z coordinates of the most stable clusters reported in ref 15 and for useful discussions during the realization of this work. We thank DGSCA-UNAM Supercomputer Center for valuable computer resources used in this research. This work was supported by DGAPA-UNAM under Projects IN106408 and IN112808. Partial financial support from 80610 is acknowledged.

Supporting Information Available: Files of the x, y, z coordinates of the calculated structures presented in Figure 1 and figures with total and partial electronic density of states of the C_1 and C_3 isomers of the Au_{34}^-cluster. This material is available free of charge via the Internet at http://pubs.acs.org.

References and Notes

(1) (a) Pyykkö, P. *Angew. Chem., Int. Ed.* **2004**, *43*, 4412. (b) Pyykkö, P. *Inorg. Chim. Acta* **2005**, *358*, 4113. (c) Baletto, F.; Ferrando, R. *Rev. Mod. Phys.* **2005**, *77*, 371.

(2) Furche, F.; Ahlrichs, R.; Weis, P.; Jacob, C.; Gilb, S; Bierweiler, T.; Kappes, M. M. *J. Chem. Phys.* **2002**, *117*, 6982.

(3) Häkkinen, H.; Yoon, B.; Landman, U.; Li, X.; Zhai, H. J.; Wang, L. S. *J. Phys. Chem. A* **2003**, *107*, 6168.

(4) Häkkinen, H.; Moseler, M.; Kostsko, O.; Morgner, N.; Hoffmann, M. A.; Issendorff, B. v. *Phys. Rev. Lett.* **2004**, *93*, 093401.

(5) Xing, X.; Yoon, B.; Landman, U.; Parks, J. H. *Phys. Rev. B* **2006**, *74*, 165423.

(6) Bulusu, S.; Li, X.; Wang, L. S.; Zeng, X. C. *Proc. Natl. Acad. Sci. U.S.A.* **2006**, *103*, 8326.

(7) Li, J.; Li., X.; Zhai, H. J.; Wang, L. S. *Science* **2003**, *299*, 864.

(8) Yoon, B.; Koskinen, P.; Huber, P.; Kostsko, B.; Issendorff, B.v.; Häkkinen, H.; Moseler, M.; Landman, U. *ChemPhysChem* **2007**, *8*, 157.

(9) Bulusu, S.; Li, X.; Wang, L. S.; Zeng, X. C. *J. Phys. Chem. C.* **2007**, *111*, 4190.

(10) Gu, X.; Ji, M.; Wei, S. H.; Gong, X. G. *Phys. Rev. B* **2004**, *70*, 205401.

(11) Johansson, M. P.; Sundholm, D.; Vaara, J. *Angew. Chem., Int. Ed.* **2004**, *43*, 2678.

(12) Ji, M.; Gu, X.; Li, X.; Gong, X. G.; Li, J.; Wang, L. S. *Angew. Chem., Int. Ed.* **2005**, *44*, 7119.

(13) Jalbout, A. F.; Contreras-Torres, F. F.; Pérez, L. A.; Garzón, I. L. *J. Phys. Chem. A* **2008**, *112*, 353.

(14) Lechtken, A.; Schooss, D.; Stairs, J. R.; Blom, M. N.; Furche, F.; Morgner, N.; Kostko, O.; Issendorff, B.v.; Kappes, M. M. *Angew. Chem., Int. Ed.* **2007**, *46*, 2944.

(15) Gu, X.; Bulusu, S.; Li, X.; Zeng, X. C.; Li, J.; Gong, X. G.; Wang, L. S. *J. Phys. Chem. C* **2007**, *111*, 8228.

(16) Compounds in any C_n (n = 1, 2. .) rotational symmetry group are always chiral, see for example: Carter, R. L. *Molecular Symmetry and Group Theory*; John Wiley and Sons: New York, 1998.

(17) Garzón, I. L.; Reyes-Nava, J. A.; Rodríguez-Hernández, J. I.; Sigal, I.; Beltrán, M. R.; Michaelian, K. *Phys. Rev. B* **2002**, *66*, 073403.

(18) Garzón, I. L.; Beltrán, M. R.; González, G.; Gutiérrez-González, I.; Michaelian, K.; Reyes-Nava, J. A.; Rodríguez-Hernández, J. I. *Eur. Phys. J. D* **2003**, *24*, 105.

(19) Román-Velázquez, C. E.; Noguez, C.; Garzón, I. L. *J. Phys. Chem. B* **2003**, *107*, 12035.

(20) Schaaff, T. G.; Whetten, R. L. *J. Phys. Chem. B* **2000**, *104*, 2630.

(21) Yao, H. *Curr. Nanoscience* **2008**, *4*, 92.

(22) López-Lozano, X.; Pérez, L. A.; Garzón, I. L. *Phys. Rev. Lett.* **2006**, *97*, 233401.

(23) Garzón, I. L.; Michaelian, K.; Beltrán, M. R.; Posada-Amarillas, A.; Ordejón, P.; Artacho, E.; Sánchez-Portal, D.; Soler, J. M. *Phys. Rev. Lett.* **1998**, *81*, 1600.

(24) Soler, J. M.; Beltrán, M. R.; Michaelian, K.; Garzón, I. L.; Ordejón, P.; Sánchez-Portal, D.; Artacho, E. *Phys. Rev. B* **2000**, *61*, 5711.

(25) Fernández, E. M.; Soler, J. M.; Garzón, I. L.; Balbás, L. C. *Phys. Rev. B* **2004**, *70*, 165403.

(26) Soler, J. M.; Artacho, E.; Gale, J. D.; García, A.; Junquera, J.; Ordejón, P.; Sánchez-Portal, D. *J. Phys.: Condens. Matter* **2002**, *14*, 2745.

(27) Troullier, N.; Martins, J. L. *Phys. Rev. B* **1991**, *43*, 1993.

(28) Perdew, P.; Burke, K.; Ernzerhof, M. *Phys. Rev. Lett.* **1996**, *77*, 3865.

(29) Fernández, E. M.; Soler, J. M.; Balbás, L. C. *Phys. Rev. B* **2006**, *73*, 235433.

(30) Olson, R. M.; Gordon, M. S. *J. Chem. Phys.* **2007**, *126*, 214310.

(31) Barron, L. D. *Molecular Light Scattering and Optical Activity*; Cambridge University Press: Cambridge, 2004.

(32) Autschbach, J.; Ziegler, T.; Gisbergen, S. J. A. v.; Baerends, E. J *J. Chem. Phys.* **2002**, *116*, 6930, and references cited therein.

(33) Crawford, T. D. *Theor. Chem. Acc.* **2006**, *115*, 227.

(34) Machón, M.; Reich, S.; Thomsen, C.; Sánchez-Portal, D.; Ordejón, P. *Phys. Rev. B* **2002**, *66*, 155410.

(35) Hidalgo, F. ; Sánchez-Castillo, A.; Noguez, C. To be submitted.

(36) The cluster geometries of the corresponding 9 isomers for the neutral Au_{34} and the cationic Au_{34}^+ clusters are not displayed because they do not show differences with respect to those of the Au_{34}^- cluster, within the scale of the structures shown in Figure 1.

(37) The C_{3v} (fcc) isomer of the Au_{34}^- cluster was obtained by the local relaxation of a structure based on the truncated octahedron (fcc) 38 atom gold cluster, in which one of their hexagonal planes with 7 atoms was removed. The 34 atom cluster was obtained by placing three additional atoms on the corresponding positions to generate the fcc structure. (See lower panel of Figure 3.) This isomer was considered in ref 14 as the precursor of C_3 with a difference in energy of 0.96 eV between each other.

(38) Gautier, C.; Bürgi, T. *J. Am. Chem. Soc.* **2006**, *128*, 11079.

(39) Zhu, M.; Aikens, C. M.; Hollander, F. J.; Schatz, G. C.; Jin, R. *J. Am. Chem. Soc.* **2008**, *130*, 5883.

(40) Iwasa, T.; Nobusada, K. *J. Phys. Chem. C* **2007**, *111*, 45.

(41) Häkkinen, H.; Walter, M.; Grönbeck, H. *J. Phys. Chem. B* **2006**, *110*, 9927.

(42) Crassous, J.; Rivera, J.; Fender, N. S.; Shu, L.; Echegoyen, L.; Thilgen, C.; Herrmann, A.; Diederich, F. *Angew. Chem., Int. Ed.* **1999**, *38*, 1613.

(43) Yao, H.; Miki, K.; Nishida, N.; Sasaki, A.; Kimura, K. *J. Am. Chem. Soc.* **2005**, *127*, 15536.

(44) Yanagimoto, Y.; Negishi, Y.; Fujihara, H.; Tsukuda, T *J. Phys. Chem. B* **2006**, *110*, 11611.

(45) Gautier, C.; Bürgi, T. *J. Am. Chem. Soc.* **2008**, *130*, 7077.

(46) Huang, W.; Ji, M.; Dong, C.-D.; Gu, X.; Wang, L.-M.; Gong, X. G.; Wang, L. S. *ACS Nano* **2008**, *2*, 897.

(47) Garzón, I. L.; Posada-Amarillas, A. *Phys. Rev. B* **1996**, *54*, 11796.

(48) Doye, J. P. K.; Wales, D. J. *New J. Chem.* **1998**, *22*, 733.

(49) Michaelian, K.; Rendón, N.; Garzón, I. L. *Phys. Rev. B* **1999**, *60*, 2000.

(50) Darby, S.; Mortiner-Jones, T. V.; Johnston, R. L.; Roberts, C. *J. Chem. Phys.* **2002**, *116*, 1536.

(51) Dong, Y.; Springborg, M. *J. Phys. Chem. C* **2007**, *111*, 12528.

(52) Kartunnen, A. J.; Linnolahti, M.; Pakkanen, T. A.; Pyykkö, P. *Chem. Commun.* **2008**, *4*, 465.

JP806080B